

AIAA'88

AIAA-88-4372

Application of Dynamical Systems Theory to Nonlinear Aircraft Dynamics

Craig C. Jahnke and Fred E. C. Culick
California Institute of Technology
Pasadena, CA

AIAA Atmospheric Flight Mechanics Conference
August 15-17, 1988
Minneapolis, Minnesota

APPLICATION OF DYNAMICAL SYSTEMS THEORY
TO NONLINEAR AIRCRAFT DYNAMICS

Craig C. Jahnke* and Fred E. C. Culick**
California Institute of Technology
Pasadena, California 91125

ABSTRACT

Dynamical systems theory has been used to study nonlinear aircraft dynamics. A six degree of freedom model that neglects gravity has been analyzed. The aerodynamic model, supplied by NASA, is for a generic swept wing fighter and includes nonlinearities as functions of the angle of attack. A continuation method was used to calculate the steady states of the aircraft, and bifurcations of these steady states, as functions of the control deflections. Bifurcations were used to predict jump phenomena and the onset of periodic motion for roll coupling instabilities and high angle of attack maneuvers. The predictions were verified with numerical simulations.

List of Symbols

a - angle of attack
b - wing span
B - sideslip angle
c - wing chord
da - aileron deflection
de - elevator deflection
dr - rudder deflection
g - gravity
 I_x - inertia about roll axis
 I_y - inertia about pitch axis
 I_z - inertia about yaw axis
l - roll moment
m - pitch moment
n - yaw moment
 θ - pitch angle
 β - roll angle
p - roll rate
q - pitch rate
Q - dynamic pressure
r - yaw rate
S - wing surface area
T - thrust
 ψ - yaw angle
V - aircraft speed
W - aircraft weight
X - force along aircraft x-axis
Y - force along aircraft y-axis
Z - force along aircraft z-axis

I. INTRODUCTION

Nonlinear flight dynamics became important with the introduction of high speed, highly maneuverable pursuit aircraft in the 1940's. Inertial coupling of the lateral and longitudinal motions created instabilities that resulted in high tail loads and a loss of aircraft. Phillips' analysis of 1948 [1] showed that aircraft with low inertia in roll could experience inertial instabilities in pitch or yaw for certain critical roll rates.

Much of the subsequent research was devoted to

calculating the maximum tail loads caused by the roll coupling instability. That result required estimating the maximum angles of sideslip and attack during the instability [2,3]. The work led to the discovery that the roll coupling instability resulted in a jump of the state of the aircraft from one steady state to another [4]. A jump occurred when the state of the aircraft became unstable.

The steady states of an aircraft, and their stability, are continuous functions of the control surface deflections, so curves of steady states can be calculated as functions of the aileron, elevator, and rudder deflections. Changes in the stability of the steady states along those curves signify critical control surface deflections which cause instabilities. The roll coupling problem was thoroughly analyzed by calculating the steady states of an aircraft and their changes of stability in reference [5].

The benefit of calculating the steady states of an aircraft is the global nature of the results. Steady states can be calculated for a range of control surface deflections and will show the qualitative response of the aircraft for various control surface deflections. The ability to predict the qualitative response of the aircraft for all control surface deflections will be very useful for designing control laws. Control laws could be designed to take advantage of the qualitative differences in the response of the aircraft in different flight regimes.

Numerical simulations are useful for studying nonlinear aircraft behavior, but many must be run to provide qualitative information about the response of the aircraft. Only one specific case can be studied at a time, and it is practically impossible to simulate all possible control surface deflections. One is never sure if the response of the aircraft would be qualitatively similar for slightly different control surface deflections unless the simulation is run. Numerical simulations are very useful when used in conjunction with an analysis of the steady states of the aircraft. They can be used to explore regions of instability that were discovered by analyzing the steady states of the aircraft.

The nonlinearity of the equations of motion makes it difficult to determine the steady states of an aircraft analytically. The equations of motion must be simplified to study one type of motion or expensive iterative schemes must be used [6]. The roll coupling problem has typically been studied using a five degree of freedom model that neglects the influence of gravity and assumes constant speed [7]. Few studies have attempted to analyze the steady states for high angle of attack maneuvers because of the difficulty of determining the steady states of the necessarily more complex models.

* Graduate Student, Aeronautical Engineering
** Professor, Jet Propulsion and Mechanical Engineering; Fellow AIAA

The introduction of continuation methods made it possible to determine the steady states of the full equations of motion relatively quickly [8]. Continuation methods are numerical techniques for calculating the steady states of systems of ordinary differential equations as a function of one of the parameters of the system. Thus, the steady states of an aircraft can be calculated as functions of the aileron, elevator, and rudder deflections.

The steady states of an aircraft can be analyzed by determining their stability as functions of the control surface deflections. A change in the stability of a steady state causes the aircraft to jump from that steady state to a new stable motion. The new motion can be another steady state or a time dependent motion. For example, increasing the aileron deflection might cause an instability that results in a jump from steady to periodic motion. The result of an instability can be predicted by using dynamical systems theory. Dynamical systems theory provides rules for classifying instabilities and predicts the effects of each type of instability.

In this work we analyze the roll coupling instability and high angle of attack aircraft dynamics by analyzing the steady states of an aircraft. The results obtained for the roll coupling problem show how easy it is to analyze inertial nonlinearities by studying the steady states of an aircraft. The analysis of high angle of attack maneuvers shows the ability to predict the onset of large amplitude motions. Instabilities are located for each type of motion and the results of these instabilities are predicted. Numerical simulations are used to verify the predictions.

II. THEORETICAL BACKGROUND

2.1 Dynamical Systems Theory

Dynamical systems theory is a relatively new field and has not been widely used to study the equations of motion for an aircraft. Many systems have been studied using dynamical systems theory. The forced Duffing oscillator has been extensively studied and bifurcations, periodic motions, and chaotic motions have been predicted and verified. The essential ideas of dynamical systems theory used in this report are introduced in the following paragraphs.

Dynamical systems theory is a methodology for studying systems of ordinary differential equations. The procedure involves calculating the steady states of the system and their stability as functions of the parameters of the system. The stability of a steady state is determined by linearizing the system about the steady state and calculating the eigenvalues. A steady state is stable if the real parts of all eigenvalues are negative. The state of the system will be attracted to stable steady states and repelled from unstable steady states.

Changes in the stability of a steady state occur when the parameters of the system are varied in such a way that the real parts of one or more eigenvalues change sign. Stability boundaries can be found by searching for steady states that have one or more eigenvalues with zero real parts. Changes in the stability of a steady state lead to qualitatively different responses for the system and are called bifurcations.

There are many different types of bifurcations and each type has a different effect on the response of the system. The effects of a bifurcation can be predicted by determining how many and what type of eigenvalues have zero real parts at the bifurcation. Bifurcations for which one real eigenvalue is zero lead to the creation or destruction of two or more steady states. Bifurcations for which one pair of complex eigenvalues has zero real parts lead to the creation or destruction of periodic motions. Bifurcations for which more than one real eigenvalue is zero or more than one pair of complex eigenvalues has zero real parts lead to very complex behavior and are beyond the scope of this report. Appendix A has one example of a saddle-node bifurcation for which one real eigenvalue is zero and one example of a Hopf bifurcation for which one pair of complex eigenvalues has zero real parts. More information on bifurcations can be found in reference [9].

2.2 Continuation Methods

Continuation methods rely on the fact that the steady states of a system of ordinary differential equations are continuous functions of the parameters of the system. The idea is to fix all parameters but one and trace the steady states as functions of this parameter. Figure 1 shows how the algorithm works for the saddle-node bifurcation shown in Appendix A.

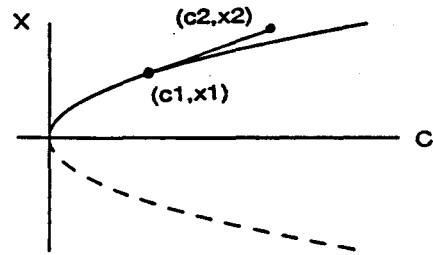


Figure 1

One steady state must initially be known, (c_1, x_1) . The slope of the curve at this point can be calculated by taking the derivative of the equation given by setting $\dot{x} = 0$. Linear extrapolation can then be used to approximate the next point on the curve, (c_2, x_2) .

The next point on the curve can also be approximated by extrapolating through two known points as shown in Figure 2. This is more efficient than the previous method as it is not

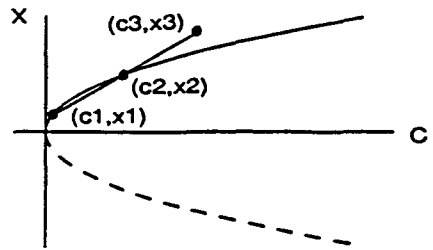


Figure 2

necessary to calculate the derivative of the system. This is especially important for large systems of equations.

Newton's method can be used to reduce the error of the approximation to an acceptable value. The whole curve of fixed points can be calculated in this manner. The stability of the steady states can be checked at each point and any change in stability will signify a bifurcation. There are other continuation method algorithms [10,11]; in this work we used the algorithm developed by Doedel and Kernevez [12].

III. MODEL OF THE AIRCRAFT DYNAMICS

The purpose of this work has been to use dynamical systems theory to analyze the equations of motion for an aircraft. The work concentrated on the roll coupling problem for several reasons. The main reason was that the roll coupling problem involved an instability that resulted in a jump in the state of the aircraft. Thus, there was good reason to believe that the instability was caused by a bifurcation of the steady states of the aircraft.

Dynamical systems theory could be used to determine if the jump was indeed caused by a bifurcation of the steady states of the aircraft. It could also be used to determine what caused the instability. The flight regimes in which the instability occurred could also be determined. The roll coupling problem also has the advantage that the effect of gravity can be neglected resulting in a simplified set of equations.

The equations of motion for an aircraft consist of:

- rotational equations

$$I_x \dot{p} = (I_y - I_z)qr + l$$

$$I_y \dot{q} = (I_z - I_x)pr + m$$

$$I_z \dot{r} = (I_x - I_y)pq + n$$

- translational equations

$$\dot{a} = q - \tan B(p \cos a + r \sin a) + \frac{1}{MV \cos B} (Z \cos a - X \sin a + W(\sin a \sin \theta + \cos a \cos \theta \cos \phi))$$

$$\dot{B} = p \sin a - r \cos a + \frac{1}{M V} (Y \cos B - X \cos a \sin B - Z \sin a \sin B + W(\cos a \sin B \sin \theta + \cos B \cos \theta \sin \phi - \sin a \sin B \cos \theta \cos \phi))$$

$$\dot{V} = \frac{1}{M} (X \cos a \cos B + Y \sin B + Z \sin a \cos B + g(\sin B \cos \theta \sin \phi + \sin a \cos B \cos \theta \cos \phi - \cos a \cos B \sin \theta))$$

- Euler angles

$$\dot{\phi} = p + \tan \theta (q \sin \phi + r \cos \phi)$$

$$\dot{\theta} = q \cos \phi - r \sin \phi$$

$$\dot{\psi} = (q \sin \phi + r \cos \phi) \sec \theta$$

This study neglected gravity which decouples Euler's equations from the rotational and translational equations. This reduces the system to six coupled

equations. Gravity has been neglected to reduce computation time, as the number of computations grows as the square of the number of equations.

The system of equations, including the aerodynamic model, used in this study is shown below. The aerodynamic model was taken from

$$p = \frac{(I_y - I_z)}{I_x} qr + \frac{1}{I_x} (B l_B + da l_{da} + dr l_{dr} + p l_p + r l_r)$$

$$q = \frac{(I_z - I_x)}{I_y} pr + \frac{1}{I_y} (m(a) + de m_{de} + q m_q)$$

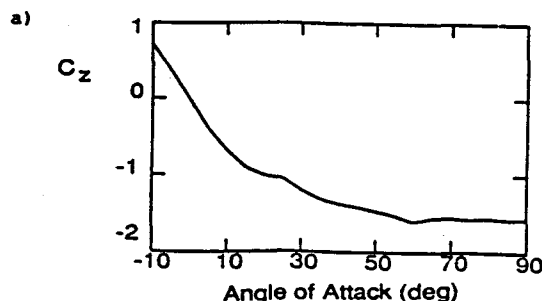
$$r = \frac{(I_x - I_y)}{I_z} pq + \frac{1}{I_z} (B n_B + da n_{da} + dr n_{dr} + p n_p + r n_r)$$

$$a = q - \tan B (p \cos a + r \sin a) + \frac{1}{MV \cos B} (-T \sin a + (Z + de Z_{de}) \cos a - (X + de X_{de}) \sin a)$$

$$B = p \sin a - r \cos a + \frac{1}{M V} ((B Y_B + da Y_{da} + dr Y_{dr} + p Y_p + r Y_r) \cos B - (X + de X_{de}) \cos a \sin B + (Z + de Z_{de}) \sin a \sin B - T \cos a \sin B)$$

$$V = \frac{1}{M} ((B Y_B + da Y_{da} + dr Y_{dr} + p Y_p + r Y_r) \sin B + (X + de X_{de}) \cos a \cos B + (Z + de Z_{de}) \sin a \cos B + T \cos a \cos B)$$

reference [13]. The model is symmetric with respect to aileron deflection and all aerodynamic coefficients are nonlinear functions of angle of attack for angles from -10 to +90 degrees. The coefficients were reported in increments of five degrees and were fitted using a cubic spline with tension. The fits of the negative lift coefficient (C_z) and the pitching moment coefficient (C_m) are shown in Figure 3. It is necessary to use a curve fit that has smooth first derivatives for convergence of the continuation method. The aerodynamic coefficients are not functions of the sideslip angle, but this could easily be added.



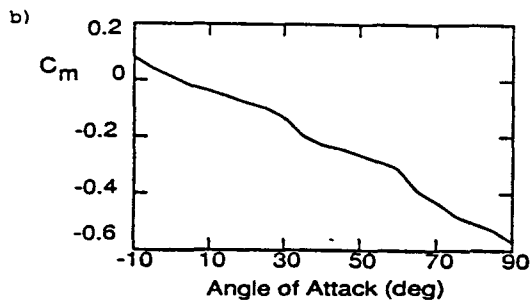


Figure 3

IV. RESULTS

4.1 Roll Coupling

We have studied the roll coupling problem by determining the steady states of the equations of motion and seeking bifurcations. The steady states are plotted as functions of the aileron setting for fixed rudder and elevator settings. The thrust to weight ratio is .12, the atmospheric density is .237 kg/m³, and the rudder deflection is zero for the results given here. Thus, the altitude is assumed constant and there is no control of yaw motion.

Figure 4 shows the steady states for a roll from the trim condition. There are six plots in Figure 4 because we are studying a six degree of freedom model; each plot shows one degree of freedom. Figure 4 also shows that there are several steady states for any aileron deflection. This can be seen by drawing a vertical line representing a constant aileron deflection on any of the plots in Figure 4. The line intersects several curves of fixed points; each intersection shows a possible steady state for the aircraft. For example, the trim condition can be found by drawing a vertical line representing zero aileron deflection on Figures 4(a)-(f). The trim condition is given by the stable steady state labelled A in Figures 4(a)-(f).

Only one branch of steady states in Figures 4(a)-(f) is stable (shown as a solid line). The other steady states, represented by dashed lines, are unstable. This convention will be used throughout the paper. Unstable steady states will not show up in flight tests or numerical simulations, as these steady states are unstable to small perturbations causing the aircraft to diverge from these states. Thus for rolls from trim only one steady state will be observed. Note that we have no information on possible time dependent motions. We are only studying steady states, that is, states with no rotational or translational accelerations.

The existence of multiple steady states can have strong consequences on the dynamics of the aircraft. While only one steady state is stable for rolls from trim (Figures 4(a)-(f)), it is possible that changing another parameter, such as the elevator deflection, could cause one of the unstable branches to become stable. There would then be two possible stable motions for the aircraft and a pilot could find himself in either type. It is very important to monitor the stability of all branches of steady states as

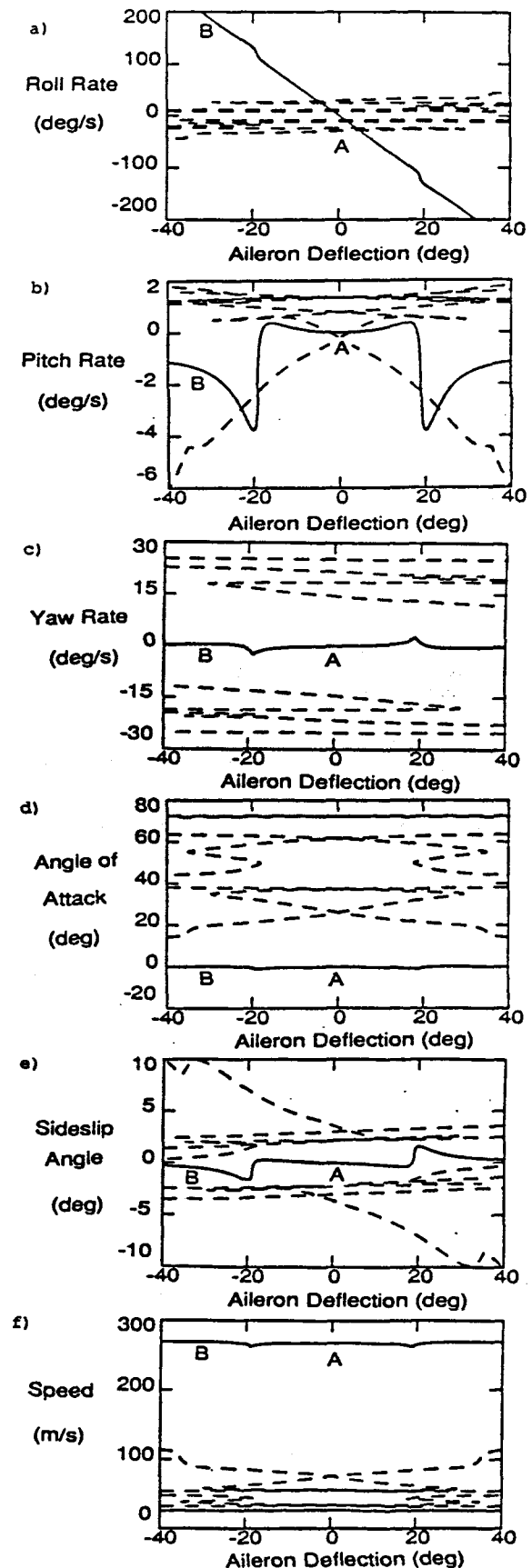


Figure 4 : Steady States For $de = 1.65$

control surface deflections or other parameters are varied. While all branches of steady states were monitored in this study, the following results show only those branches containing stable steady states.

Figure 4 shows the symmetry of the aerodynamic model with respect to aileron deflection. The longitudinal motions (Figures 4(b), (d), (f)) are symmetric with respect to the aileron deflection; positive and negative aileron deflections cause the same pitch rate, angle of attack, and speed. Lateral motions (Figures 4(a), (c), (e)) are antisymmetric with respect to aileron deflections; positive and negative aileron deflections cause roll rates, yaw rates, and sideslip angles of the same magnitude but opposite signs. Subsequent results will show only positive roll rate solutions.

Figure 5 shows the steady states for an elevator setting of 3 degrees. The elevator setting has only been increased by 1.35 degrees from the case shown in Figure 4, but there is a vast difference in the nature of the steady state solutions. The branch of stable steady states in Figure 5 contains several bifurcations; saddle-node bifurcations are labelled by circles and Hopf bifurcations are labelled by x's. The branch of stable steady states in Figure 4 did not contain any bifurcations, so there should be a qualitative difference in the response of the aircraft for rolls from trim and rolls with an elevator setting of 3 degrees.

The motion of the aircraft for rolls from trim can be inferred from Figure 4. Assume the aircraft starts from the trim condition represented by point A in Figures 4(a)-(f). Applying negative aileron deflection would cause the state of the aircraft to follow the curve of stable steady states (allowing for transient motions). Increasing the aileron deflection to -30 degrees will cause the state of the aircraft to go from point A to point B in Figures 4(a)-(f). Following the curve of steady states from A to B shows that the state of the aircraft would change in a continuous fashion.

Now perform the same maneuver for an elevator deflection of 3 degrees. As shown in Figures 5(a)-(c), for zero aileron deflection the aircraft has zero roll and yaw rates, and a negative pitch rate (pitch down maneuver). Increasing the aileron deflection from zero causes the state of the aircraft to follow the curve of stable steady states in Figures 5(a)-(f). The state of the aircraft would change continuously from state A to state B. If the aileron deflection is increased past state B the aircraft must jump to state C.

A simulation of this maneuver is shown in Figure 6. The state of the aircraft is given by Figures 6(a)-(f) and the aileron input is shown in Figure 6(g). The aileron deflection was increased enough to cause the jump from state B to state C in Figures 5(a)-(f) to occur. The jump is clearly shown in the yaw rate (Figure 6(c)) and the angle of attack (Figure 6(d)) at a time of 25 seconds.

Figures 5(c)-(d) show that as the aileron is increased from zero (point A) the yaw rate and angle of attack should both become more negative. This behavior is shown in Figures 6(c)-(d) for times from zero to 15 seconds. Figures 5(c)-(d) show that increasing the aileron deflection past the saddle-node bifurcation at point B will cause

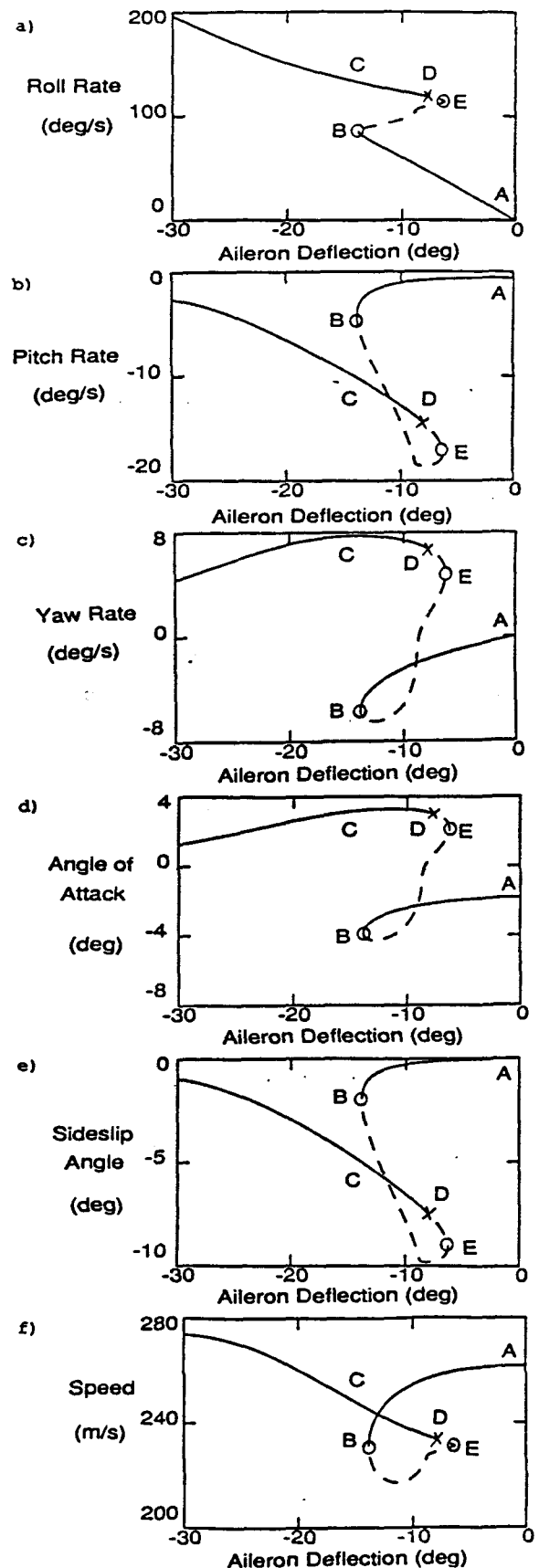


Figure 5 : Steady States For $\delta_e = 3$.

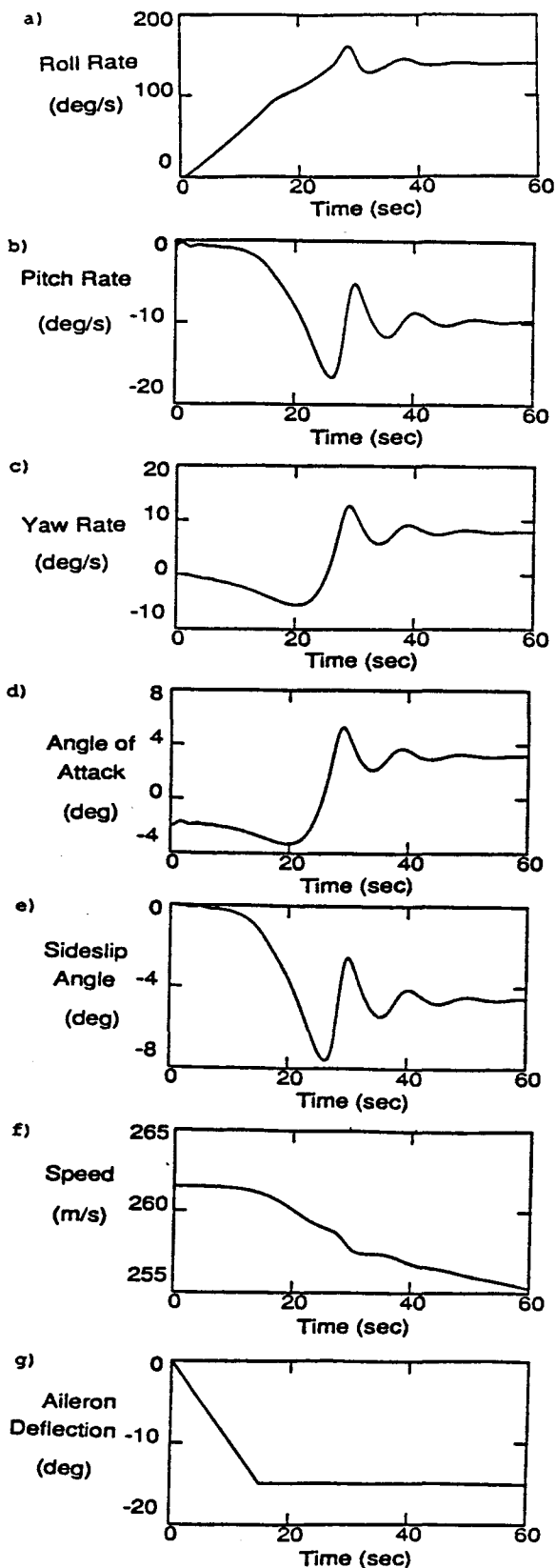


Figure 6 : Simulation For $d_e = 3$.

the yaw rate and angle of attack to jump to positive values. This jump occurs in Figures 6 (c)-(d) at a time of 25 seconds. Comparing the yaw rate and angle of attack given for state C in Figures 5(c)-(d) with the final yaw rate and angle of attack in Figures 6(c)-(d) shows that the state of the aircraft after the jump can be predicted by knowing the steady states of the aircraft.

Figure 7 shows the aileron settings which cause bifurcations, for a range of elevator deflections. The figure can be interpreted by comparing it with Figure 5. The bifurcation in Figures 5(a)-(f) (labelled B, D, E) occur at fixed aileron deflections and an elevator deflection of 3 degrees. The location of these bifurcations can be plotted as functions of elevator and aileron deflections with all other parameters held constant; points B, D, and E in Figure 7 represent the bifurcations labelled B, D, and E in Figure 5. Figure 7 shows that the control surface deflections which cause bifurcations can be plotted as continuous functions.

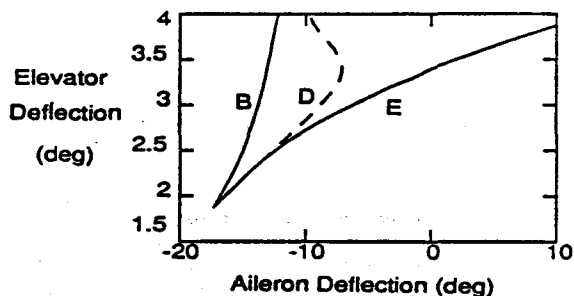


Figure 7 : Bifurcation Diagram

The jump in the state of the aircraft caused by the saddle-node bifurcation at state B in Figures 5(a)-(f) is due to inertial coupling. This can be seen by studying the individual components that compose the moments in roll, pitch, and yaw. Figure 8 shows the main contributions of inertial and aerodynamic terms to the roll, pitch, and yaw moments for a range of aileron deflections and an elevator deflection of 3 degrees (case shown in Figure 5).

Figure 8(a) shows that the roll moment caused by $d_a l_{da}$ (curve 1) is balanced by the damping in roll, $p l_p$ (curve 3) for most aileron deflections. Near the saddle-node bifurcation ($d_a = -14$) sideslip builds up causing a positive roll moment due to $B l_B$ (curve 2). For this moment to be balanced by $p l_p$ the roll rate must increase as l_p remains essentially constant as there is very little change in the angle of attack during the maneuver (see Figure 5(d)).

Figure 8(b) shows that for aileron deflections less than 5 degrees the pitching moment caused by the elevator deflection, $d_e m_{de}$ (curve 4) is balanced by the pitching moment due to angle of attack, $m(a)$ (curve 1) as would be expected for linear aircraft dynamics. For aileron settings near -14 degrees the contribution of $m(a)$ decreases very rapidly and changes sign because the angle of attack changes signs (see Figure 5(d)). The

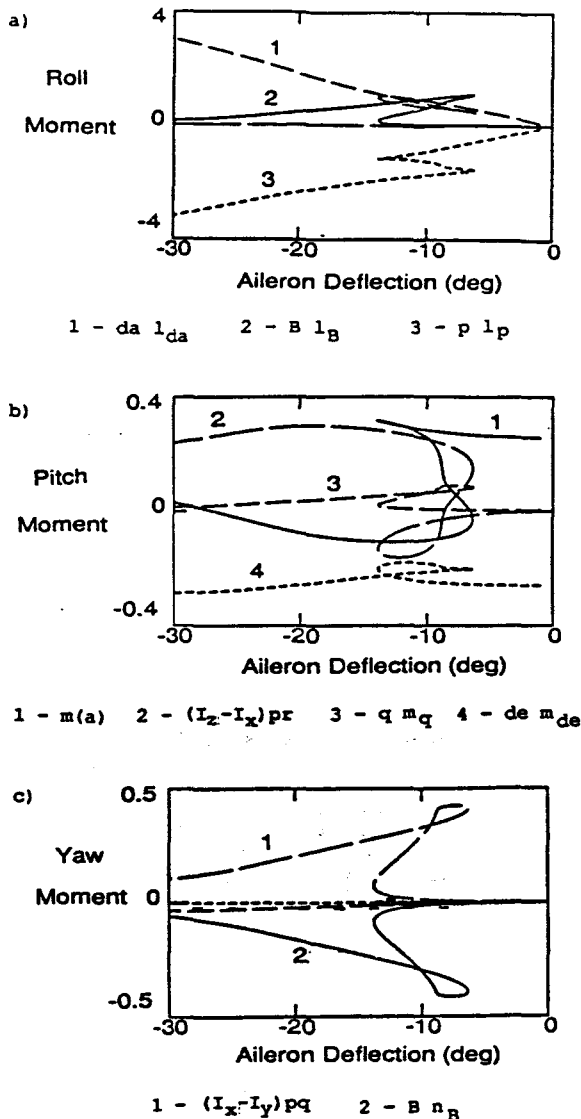


Figure 8 : Moment Contributions For $\delta_e = 3$.

decrease in $m(a)$ is accompanied by an increase in the inertial moment (curve 2). For aileron deflections greater than -14 degrees (past the saddle-node bifurcation) the main contributions to the pitching moment are $d e m_{de}$ and the inertial moment. Thus the saddle-node bifurcation changes the pitching moment balance from one dominated by aerodynamic terms (curves 1 and 4) to one composed of inertial and aerodynamic terms (curves 2 and 4).

Figure 8(c) shows that the yaw moment balance is between the inertial term (curve 1) and the directional stability term $B n_B$ (curve 2). This shows one source for the buildup of sideslip, which was shown to cause an increase in the roll rate through the term $B l_B$. As the aileron deflection is increased the roll rate increases causing the inertial term (curve 1) to increase. For this moment to be balanced the sideslip angle must increase as n_B is essentially constant because the angle of attack does not change much during the maneuver.

The jump in the state of the aircraft caused by the roll coupling instability involves a complex balancing of moments. The increase in the inertial coupling moments causes the aircraft to jump from a flight regime dominated by aerodynamic moments to one involving aerodynamic and inertial moments. While no one term causes the roll coupling instability, the aerodynamic terms $m(a)$ and n_B play a large part. Changing these coefficients should have an effect on the instability. Increasing $m(a)$ would allow it to balance larger moments caused by $d e m_{de}$ and inertial coupling (see Figure 8(b)). The saddle-node bifurcation would then be moved to a larger aileron deflection.

Similarly by increasing n_B less sideslip would be needed to balance the inertial moment in yaw (see Figure 8(c)). Thus less roll rate would be needed to balance the roll moment caused by $B l_B$ (see Figure 8(c)) and less inertial moment in pitch would buildup. Again the effect would be to allow larger aileron deflections before the saddle-node bifurcation would occur.

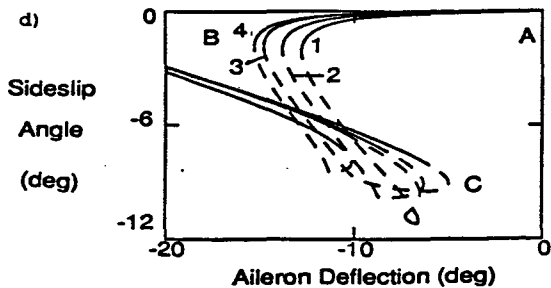
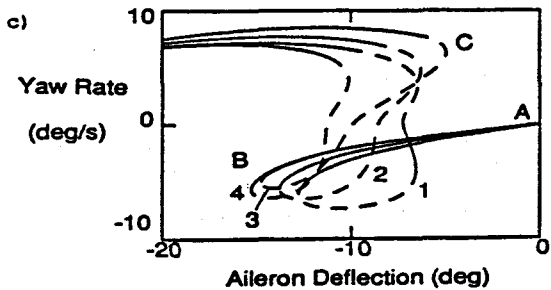
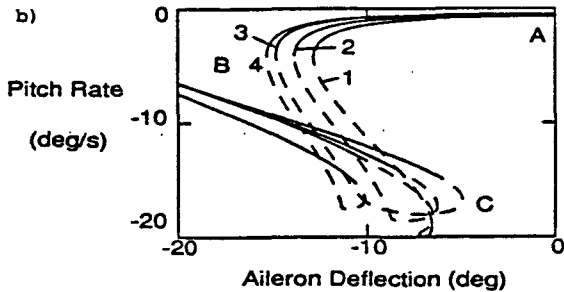
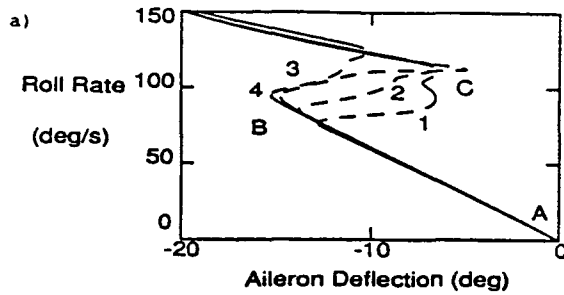
Figures 9(a)-(d) show the effect of changing $m(a)$ and n_B on the steady states of the aircraft for an elevator setting of 3 degrees (cf. Figure 8). Changing these coefficients has little effect on the steady states of the aircraft for large or small aileron deflections. The main effect occurs between the saddle-node bifurcations (B and C) where inertial forces start to become important.

Figure 9(a) shows that increasing $m(a)$ increases the aileron deflection where the saddle-node bifurcation occurs. This allows higher roll rates to be achieved before the bifurcation occurs. Figures 9(b)-(d) show that increasing $m(a)$ and n_B reduces the buildup of pitch rate, yaw rate, and sideslip for aileron deflections less than those required for the bifurcation to occur (i.e. between points A and B).

The effect of changing $m(a)$ and n_B on the critical control deflections which cause the two saddle-node bifurcations (shown as solid lines) in Figure 7 is shown in Figure 10. Curve 2 in Figure 10 is the same curve shown in figure 7. The curves show that increasing $m(a)$ and n_B allows larger aileron deflections before a saddle-node bifurcation occurs for a range of elevator deflections.

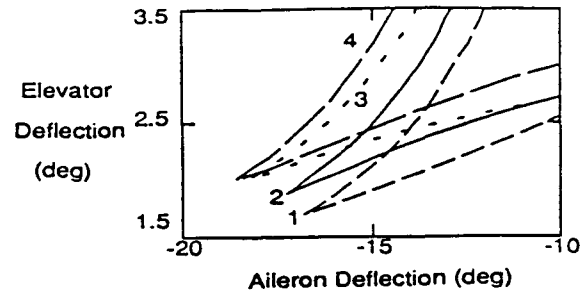
Figure 11 shows the steady states for an elevator deflection of 4 degrees. A comparison of Figures 5 and 11 shows that increasing the aileron deflection from 3 to 4 degrees leads to very different steady states. In particular Figure 11 has two separate branches of steady states, while Figure 5 has only one. This can easily be seen by comparing Figures 5(d) and 11(d). Thus one of the unstable branches of steady states shown in Figure 4 becomes stable as the elevator deflection is increased from 1.65 to 4 degrees.

The effect of the Hopf bifurcation at state 4 in Figures 11(a)-(f) can be seen in the simulation shown in Figure 12. The maneuver can be understood by comparing Figures 11(a)-(f) with Figures 12(a)-(g). The simulation starts from state 1 in Figures 11(a)-(f). When the aileron deflection is increased up to and past state 2 the state of the aircraft must jump to state 3. The effect of this jump can be seen particularly well in the sudden jump in the yaw rate and angle of attack at a time of 15 seconds in Figures 12(c)-(d).



- 1 - $m(a) \rightarrow .9 m(a)$
- 2 - $m(a)$
- 3 - $m(a) \rightarrow 1.1 m(a)$
- 4 - $(m(a), n_B) \rightarrow (1.1m(a), 1.1n_B)$

Figure 9 : Steady States For $\delta_e = 3$.



- 1 - $m(a) \rightarrow .9 m(a)$
- 2 - $m(a)$
- 3 - $m(a) \rightarrow 1.1 m(a)$
- 4 - $(m(a), n_B) \rightarrow (1.1m(a), 1.1n_B)$

Figure 10 : Bifurcation Diagram

The aileron deflection is then decreased, as shown in Figure 12(g), causing the aircraft to go from state 3 (Figures 11(a)-(f)) through the Hopf bifurcation at state 4 and finally to state 5. The Hopf bifurcation leads to the growing oscillations seen in Figures 12(a)-(e) for times between 30 and 90 seconds. The limit cycle becomes unstable when the aileron deflection is returned to zero and the aircraft returns to its initial state.

Figures 11(a)-(f) and 12(a)-(f) show that saddle-node bifurcations also cause hysteresis type behavior. The state of the aircraft jumped from state 2 to state 3 (figure 11) when the aileron deflection was increased past state 2. When the aileron deflection was decreased from state 3 the aircraft did not jump back to state 2 but went to state 5. Only when the aileron deflection was returned to zero did the aircraft jump back to the initial branch of steady states.

4.2 High Angle of Attack Dynamics

The previous methods can also be used to study high angle of attack aircraft motion. While the present aircraft model might not be valid for high angle of attack flight, the following results show the type of information that could be obtained from a more complete model.

Figures 13(a)-(f) show the steady states of the aircraft for an elevator setting of -13 degrees. The figures show that for aileron deflections larger than about 6 degrees there are no stable steady states. For flight regimes where there are no stable steady states the aircraft must undergo some type of time dependent motion. This can be seen in the simulation in Figures 14(a)-(g).

The simulation starts with the aircraft in state A of Figure 13. The aileron deflection is increased causing the aircraft to go from state A up to and past state B. The aileron deflection is then held constant at a value just past that at state B. Figures 14(a)-(f) show that the aircraft exhibits time dependent motion when the aileron deflection is held constant at 7 degrees (i.e. for

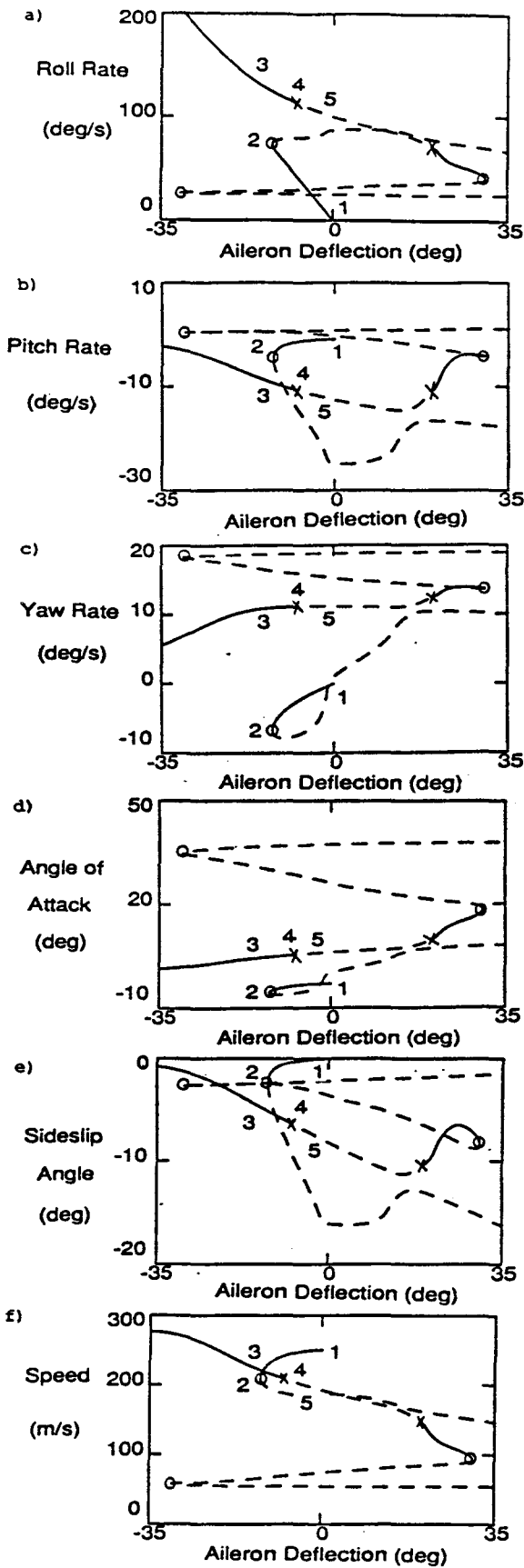


Figure 11 : Steady States For $d_e = 4$.

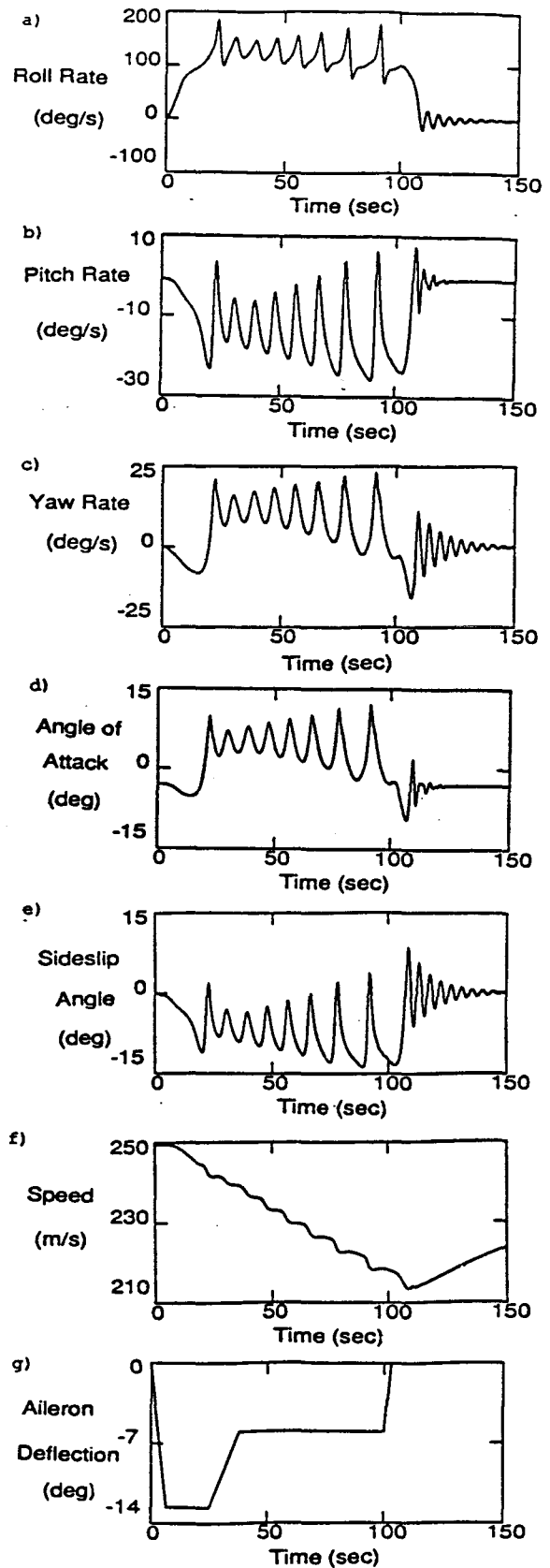


Figure 12 : Simulation For $d_e = 4$.

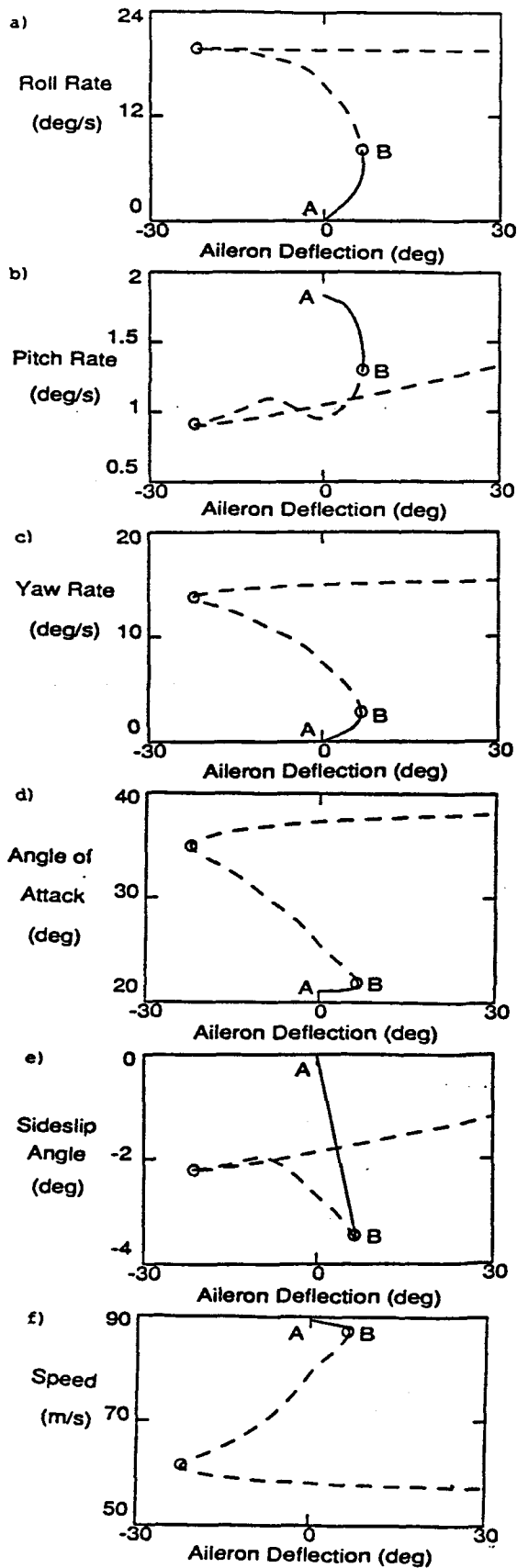


Figure 13 : Steady States For $d_e = -13$.

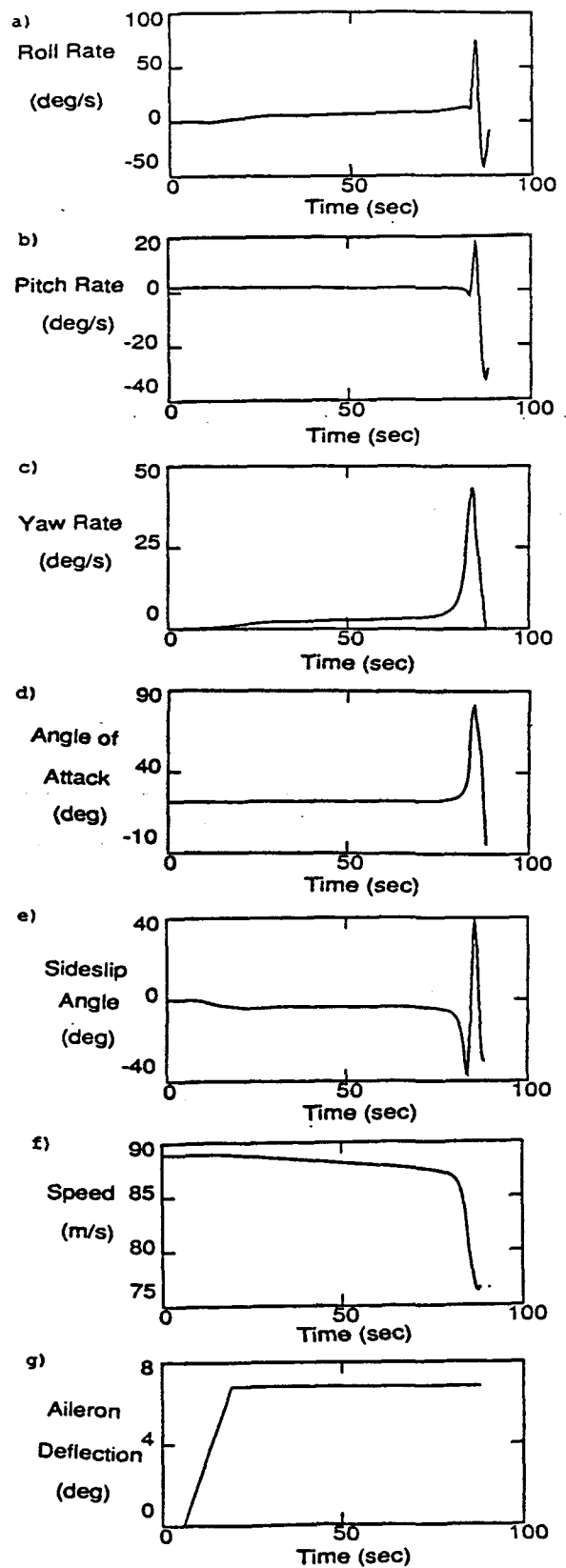


Figure 14 : Simulation For $d_e = -13$.

times greater than 20 seconds).

For times between 20 and 80 seconds there is only a slight change in the state of the aircraft. This is most apparent in the roll and yaw rates (Figures 14(a) and (c)). The aircraft undergoes a sudden violent motion at a time of 80 seconds. The magnitude of the motion is surprisingly large. The roll rate changes from 80 to -40 deg/sec in only a few seconds (Figure 14(a)). The simulation had to be stopped as the angle of attack exceeded the limit of the aerodynamic model.

It is clearly very important to know if and when this type of motion could occur. Figure 15 shows that there are curves of saddle-node and Hopf bifurcations above which no stable steady states exist. This information could be used to put limits on the control deflections or at least to show which flight regimes need further study.

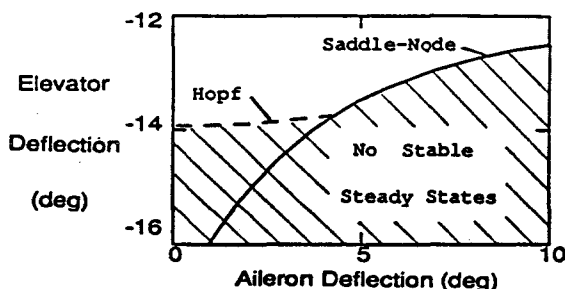


Figure 15 : Bifurcation Diagram

V. CONCLUSIONS

The above results show the value of using continuation methods and dynamical systems theory to analyze the equations of motion for an aircraft. The efficiency of the method makes it possible to study various regions of the flight envelope and look for instabilities like the roll coupling instability. It is not necessary to simplify the equations of motion to study known phenomena, so it is possible to find some unexpected phenomena.

The method also has great potential for designing control laws. Figures like Figure 6 could be made three dimensional by including rudder deflection as another variable. There would then be surfaces of control deflections which cause bifurcations. Control laws could be designed to avoid these surfaces. These surfaces would be functions of the altitude, Mach number, and thrust setting, so these variables would have to be incorporated into the control laws.

A knowledge of which control deflections cause bifurcations can also be used to escape from motions caused by a bifurcation. A pilot would know the correct control surface deflections to cause the aircraft to bifurcate back to the desired state, or knowing all the steady states of the aircraft a pilot could pick the best combination of control surface deflections to get to the desired steady state.

The above analysis can also be extended to periodic motions. It is possible to obtain curves of periodic motions as a function of the control settings similar to the curves of steady states shown in this work. Periodic motion could then be avoided by staying away from control surface deflections which cause stable periodic motions.

ACKNOWLEDGEMENTS

This work was partly supported by Caltech funds and partly by a grant from the National Aeronautics and Space Administration, Ames Dryden Flight Research Center.

REFERENCES

1. Phillips, W. H.: Effect of Steady Rolling on Longitudinal and Directional Stability. TN-1627, 1948.
2. Pinsker, W. G.: Charts of Peak Amplitudes in Incidence and Sideslip in Rolling Maneuvers Due to Inertia Cross Coupling. ARC RM No. 3293, 1962.
3. Rhoads, D. W. and Schuler, J. M.: A Theoretical and Experimental Study of Airplane Dynamics in Large Disturbance Maneuvers. Journal of Astronautical Sciences, Vol. 24, July 1957.
4. Gates, O. B. and Minka, K.: Note on a Criterion for Severity of Roll Induced Instability. Journal of Aerospace Sciences, May 1959.
5. Young, J. W., Schy, A. A., and Johnson, K. G.: Pseudosteady State Analysis of Nonlinear Aircraft Maneuvers. Proceedings of 7th AIAA Atmospheric Flight Mechanics Conference, August 11-13, 1980.
6. Adams, W. M.: Analytic Prediction of Aircraft Equilibrium Spin Characteristics. NASA TN D-6926, 1972.
7. Hacker, T. and Oprisiu, C.: A Discussion of the Roll Coupling Problem. Progress in Aerospace Sciences, Vol. 15 Pergamon Press, Oxford, 1974.
8. Guicheteau, P.: Bifurcation Theory Applied to the Study of Control Losses on Combat Aircraft. Proceedings AGARD/FMP Symposium on Combat Aircraft Maneuverability, October 5-8, 1981.
9. Guckenheimer, J. and Holmes, P.: Nonlinear Oscillations, Dynamical Systems, and Bifurcations of Vector Fields. Springer-Verlag, New York, 1983.
10. Keller, H. B.: Numerical Solution of Bifurcation and Nonlinear Eigenvalue Problems. Applications of Bifurcation Theory, Academic Press, New York 1977.
11. Kubicek, M.: Algorithm 502: Dependence Of the Solution of Nonlinear Systems on a Parameter. ACM Transactions on Mathematical Software, 2, 1976.
12. Doedel, E. J. and Kernevez, J. P.: Software for Continuation Problems in Ordinary Differential Equations With Applications. Preprint.
13. Young, J. W., Schy, A. A., and Johnson, K. G.: Steady State Analysis of Nonlinear Aircraft Maneuvers. NASA TP 1758, 1980.

APPENDIX A

The following examples show how bifurcations can be found and how they effect the response of the system. The saddle-node bifurcation is the simplest bifurcation with one zero eigenvalue. Saddle-node bifurcations cause the creation of one unstable steady state (saddle) and one stable steady state (node), hence the name saddle-node bifurcation. Saddle-node bifurcations are common in physical problems and can cause jump phenomena when the stable steady state is destroyed, as the system must jump to a new steady state or time dependent motion. The Hopf bifurcation is the simplest example of a bifurcation for which one pair of complex eigenvalues has zero real parts. Hopf bifurcations are common in physical systems and cause the creation or destruction of periodic motion.

A1. Saddle-Node Bifurcation

Consider the equation

$$\dot{x} = c - x^2$$

The steady states of this equation ($\dot{x} = 0$) are given by $x = \pm\sqrt{c}$. If c is negative there are no steady states. Linearizing the equation about the steady state $x = \sqrt{c}$ gives the equation

$$\dot{u} = -2\sqrt{c} u$$

where $u = x - \sqrt{c}$. The eigenvalue, $e = -2\sqrt{c}$, is negative so the steady state is stable. Applying the same analysis to the steady state $x = -\sqrt{c}$ shows that it is unstable. These results are plotted in Figure 16. The solid line shows the steady stable states and the dashed line the unstable steady states. The vertical lines with the arrows show the evolution of the system in time for fixed values of c and some chosen initial condition (x,c) . The arrows represent increasing time.

The system has a bifurcation at $c = 0$ as the eigenvalue at $(x,c) = (0,0)$ is zero. Thus, the system should exhibit different qualitative behaviors for c less than zero and for c greater than zero. This is clearly shown in Figure 17. For the same initial value of x the system responds differently for positive and negative values of c . If c is positive the system approaches the steady state, $x = \sqrt{c}$, shown in Figure 16. If c is negative there are no stable steady states and x continually decreases.

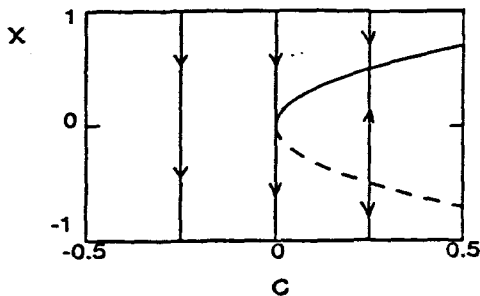


Figure 16

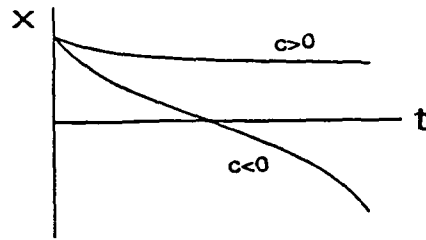


Figure 17

A2. Hopf Bifurcation

Consider the system written in polar coordinates

$$\dot{r} = r (c - r^2)$$

$$\dot{\theta} = 1$$

This system has a fixed point at the origin for all values of c and a periodic orbit, or limit cycle, for $c > 0$ given by $r = \sqrt{c}$. The system must be transformed to rectangular coordinates to calculate the eigenvalues of the the steady state $r = 0$. In rectangular coordinates the system is given by

$$\dot{x} = c x - y - x (x^2 + y^2)$$

$$\dot{y} = c y + x - y (x^2 + y^2)$$

linearizing about the origin gives the system

$$\begin{pmatrix} \dot{x} \\ \dot{y} \end{pmatrix} = \begin{bmatrix} c & -1 \\ 1 & c \end{bmatrix} \begin{pmatrix} x \\ y \end{pmatrix}$$

which has eigenvalues $e = c \pm i$, where $i = \sqrt{-1}$. The origin is stable for $c < 0$ and unstable for $c > 0$. For $c = 0$ the eigenvalues at the origin are purely imaginary. Thus, the origin undergoes a Hopf bifurcation for $c = 0$ which creates the limit cycle $r = \sqrt{c}$. This is shown in figure 18.

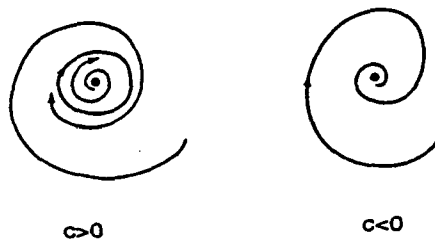


Figure 18